Int. J. Electrochem. Sci., 11 **(2016)** 6688 – 6695, doi: 10.20964/2016.08.40

International Journal of
ELECTROCHEMICAL
SCIENCE
www.electrochemsci.org

Short Communication

Electrochemical Performance of Activated Carbons with Different Specific Surface Area as Supercapacitor Electrode Materials

Wei Wang[1], *Fanghua Zhu*[2,*], *Wei Jia*[1], *Yan Wu*[1], *Liming Zhao*[1], *Liang Yu*[1], *Yalei Chen*[1], *Zhen Shen*[1]

[1] School of Materials Science and Engineering, Southwest University of Science and Technology, Mianyang 621010, China.
[2] Research Center of Laser Fusion, China Academy of Engineering Physics, Mianyang, Sichuan 621900, China.
[*]E-mail: fanghuazhu@sina.com

Received: 18 March 2016 / *Accepted:* 23 May 2016 / *Published:* 7 July 2016

In this paper, we chose commercial activated carbons (AC) as electrode materials because the advantage of abundant in raw, lower price and larger specific surface area. First, we characterized the physical properties of these two ACs. Second, we utilized these ACs to prepare electrode as working electrodes and characterized in the 1 mol/L H_2SO_4, The results indicated that the specific surface of 1-AC and 2-AC are 758 m^2/g and 1771 m^2/g respectively. The tests of electrochemical capacitance performance indicated that the specific capacitance of electrode increased with the specific surface area increasing. And both electrochemical stability retained over 90% of the original capacitance.

Keywords: activated carbon; supercapacitor; electrode material

1. INTRODUCTION

Supercapacitors are also known as electrochemical capacitors or ultracapacitors, which are the energy storage devices between the batteries and the traditional dielectric capacitors [1,2]. The supercapacitor has a higher energy density than traditional capacitor and a greater power density than battery, which can be used as a single energy storage element, and can be connected to the battery in parallel to form a composite power supply system [3]. Supercapacitor in the new energy power generation, electric vehicles, defense technology and aerospace and other fields have broad application prospects.

The properties of electrode materials are very important in the supercapacitor, which is directly related to the performance of the capacitor [4]. Carbon electrode materials for research is now focused on activated carbon (AC), carbon nanotubes, carbon fiber, graphene, and composite material on, because carbon materials is the earliest found and most mature, the only one of the industrialization of the products [5-7]. Now research mainly concentrated on improving the direction of the capacitance density and energy density.

The high specific surface area and high conductivity carbon material is the first choice of the electrode material of the supercapacitor, the specific surface area of the carbon material directly determines its electrochemical capacitance performance. Largeot *et al.*[8] prepare AC with pore size control by using TiC-carbon derivative system. The AC pore size of the average pore size control in the 0.65~1.1 nm, and with different chlorination temperature were prepared with different specific surface area of AC. They found that the maximum capacitance of the aperture is close to the size of the ion, too large and too small aperture will cause a reduction in the ratio of the capacitor. Liu *et al.*[9] first use biological crab as template to prepare highly ordered mesoporous carbon fiber, with the ratio of surface area up to 1270 m^2 / g, and applied it as supercapacitor electrode.

In this study, two kinds of ACs were selected as electrode materials and their physical and electrochemical properties were characterized. The results of electrochemical capacitance performance indicated that the specific capacitance of electrode increased from 758 m^2/g to 1771 m^2/g with the specific surface area of AC increasing. And both electrochemical stabilites of them were retained over 90% of the original capacitance.

2. EXPERIMENTAL

2.1. Chemicals

ACs (600~800 m^2/g and 1700~1900 m^2/g) were purchased from Merck Chemical Reagent Company. Sulfuric acid, acetone and ethanol were purchased from Chengdu Kelong Chemical Reagent Factory.

2.3. Characterizations

Fourier transform infrared spectra (FTIR) of these samples were recorded on a spectrometer (Nicolet-5700, USA) using pressed KBr pellets. The morphology of the samples was observed by field-emission scanning electron microscopy (FESEM; Ultra 55). Nitrogen adsorption-desorption isotherms were measured at 77 K using a QuantachromeAutosorb-1MP analyzer.

Cyclic voltammetry (CV) tests were measured in a potential range between -1 and 0 V (vs. Hg/HgO) at various scan rates, and the charge–discharge processes were performed in the potential window from -1 and 0 V at different current densities. Electrochemical impedance spectroscopy (EIS) was carried out on an electrochemical workstation (IM6, Germany) in the frequency range from 0.1 Hz to 100 kHz with 5 mV amplitude at open circuit potential.

3. RESULTS AND DISCUSSION

3.1. SEM measurement

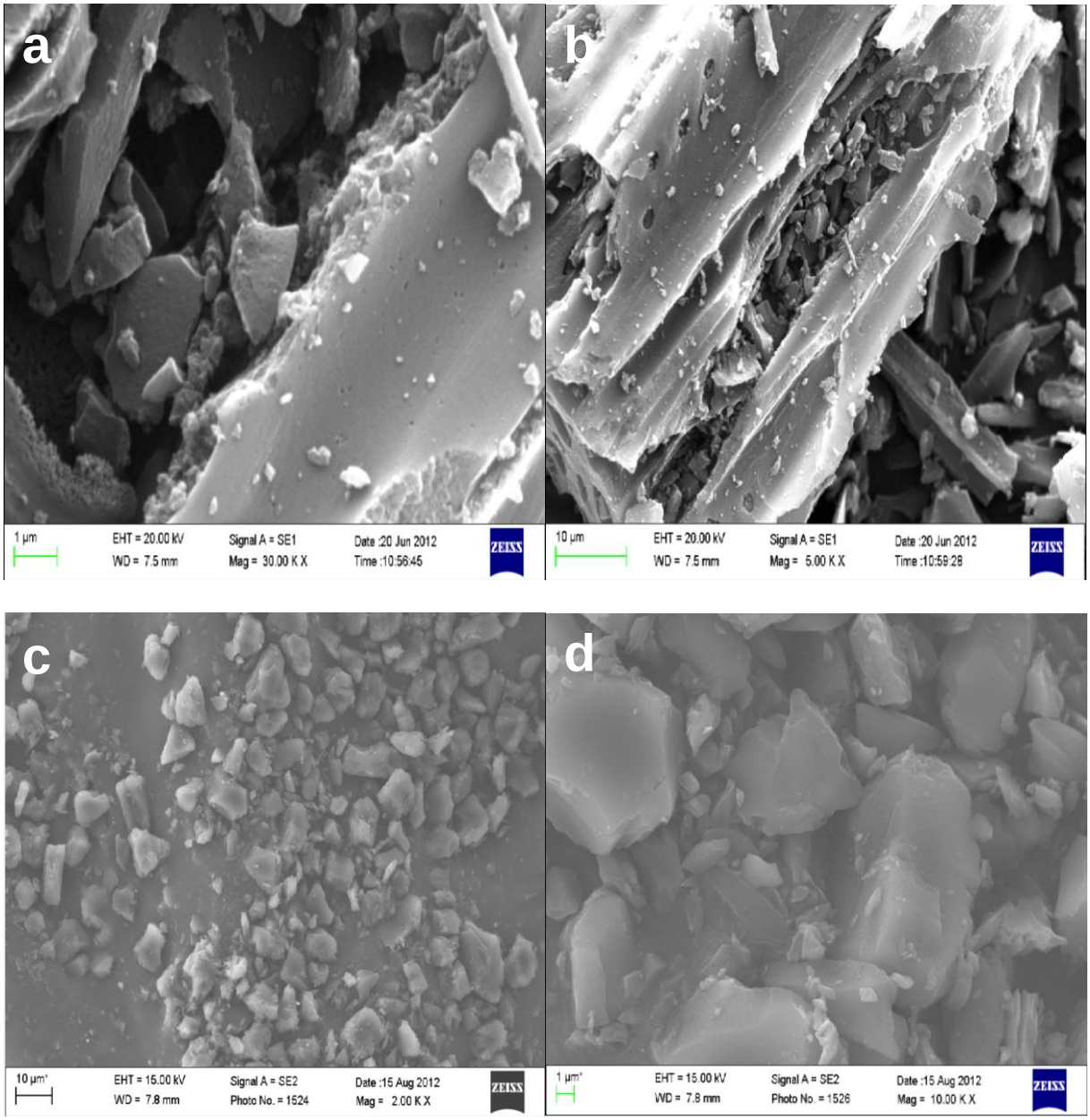

Figure 1. SEM images of 1-AC (a,b) and the 2-AC (c,d).

Figure 1 illustrates the morphologies and structures of the 1-AC (a,b) and 2-AC (c,d). From Figure1 (a, b) we can see that the size distrbution of 1-AC appears from 500 nm to 10 μm, and 1 μm pores could be observed on the surface. As can be seen from Figure1 (c, d), the 2-AC shows bulk structure, and the size distribute from 6 μm to 10 μm.

3.2. FTIR spectra

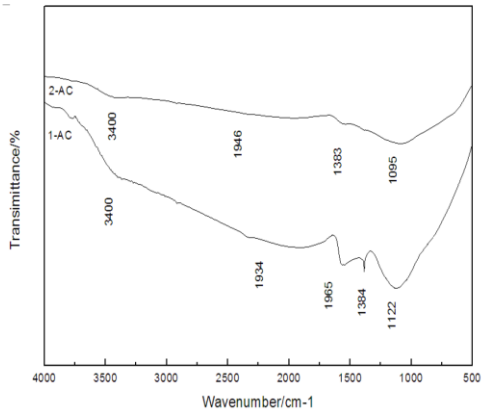

Figure 2. FTIR spectra of the 1-AC and 2-AC.

Figure 2 shows the FTIR spectrums of 1-AC and 2-AC. More infrared absorption peaks was observed of 1-AC than that of 2-AC, which may be attribute to more functional groups on 1-AC surface. A weak absorption peak appears at 3400 cm^{-1}, which may be attributed to –OH on the surface of 1-AC. The absorption peaks at 1565 cm^{-1} can be assigned to the COO- asymmetric stretching vibration. And the RC=O stretching vibration peak could be observed at 1934 cm^{-1}, the C-O stretching vibration could be recognized at 1122 cm^{-1}. The -OH absorption peak of 2-AC is weaker than that of 1-AC, and the absorption peak at 1095 cm^{-1} belongs to C-O.

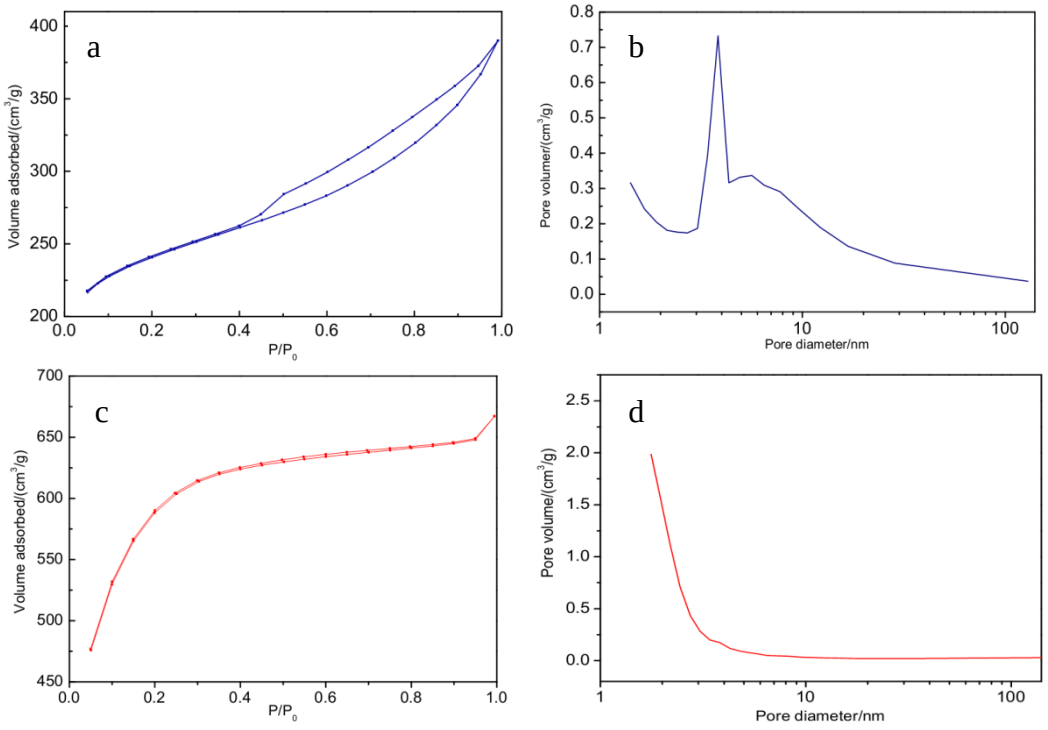

Figure 3. N_2 adsorption/desorption isotherm and the pore size distribution of 1-AC (a, b) and 2-AC (c, d).

As can be seen from Figure 3, the N_2 adsorption/desorption isotherm and the pore size distribution of the ACs were illustrated. Figure 3 (a, b) show that the adsorption isotherm of 1-AC was a typical type IV, which was generated from the mesoporous solid. It is characterized by that the adsorption curve and desorption curve of isothermal curve are not consistent. A H_3 type hysteresis loops can be observed, and there was no restriction of adsorption at the higher pressure region. The average pore diameter is 3.81 nm, and the surface area to volume ratio was calculated to be 758 m^2/g. As illustrated from Figure 3 (c, d), the adsorption curve of 2-AC was type I nitrogen adsorption isotherm. A rapid increase was observed in adsorption volume at low pressure area, due to the filling of the pores. Adsorption curve can also be seen that there was a not obvious hysteresis loop, which belongs to the H_4 type and appears only in the solid with a narrow slit hole. The hysteresis loop of 2-AC illustrates a mesoporous range from 1 to 2 nm, indicating the surface area to volume ratio to be 1771 m^2/g.

3.3. CV curves of 1-AC and 2-AC electrodes

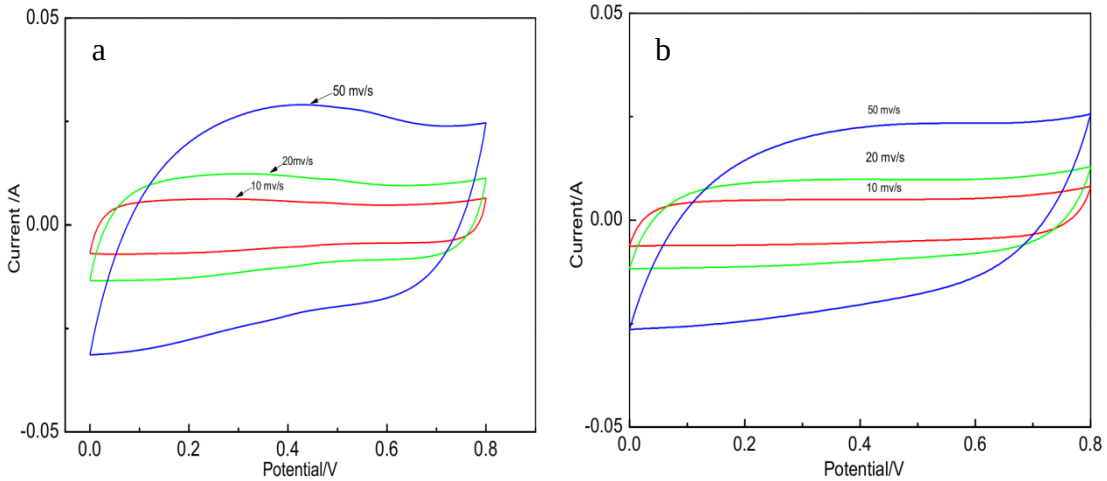

Figure 4. The CV profiles of the 1-AC (a) and the 2-AC (b) electrode at the different scan rate.

Figure 4 shows the CV curves of 1-AC and 2-AC electrodes at different scanning rates. As can be seen from Figure 4, the CV curves of the two electrodes were close to the rectangle, indicating double layer capacitance characteristics of the ACs. A wide redox peak of 1-AC was observed at 0~0.4V, which may be distributed to the reversible redox reaction of the 1-AC surface with more oxygen containing functional groups [10]. Meanwhile, the CV curve of 2-AC is more rules, and no obvious redox peak appeared. With the increase of scanning speed, the basic shape of the CV curve remains unchanged. These CV results exhibited almost rectangular curves, which corresponded to the behavior of ideal double-layer capacitance. A vertical tail in the lower-frequency domain of the Nyquist plot provided additional evidence of good supercapacitor behavior for the activated mesoporous carbons. [11]

3.4 1-AC and 2-AC electrode charge and discharge performance test

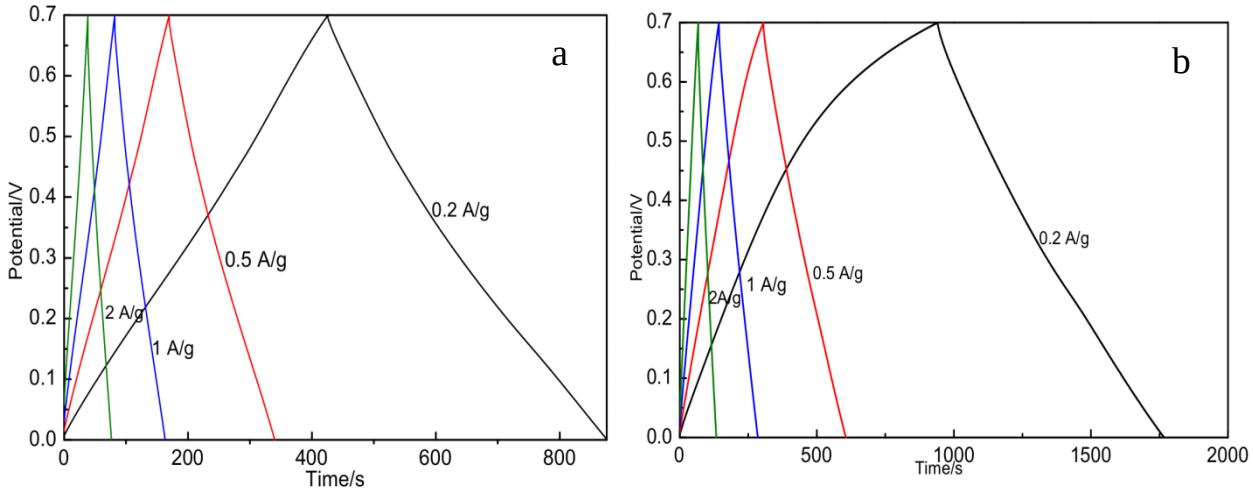

Figure 5. Galvanostatic charge/discharge curves of the 1-AC and 2-AC electrode at different current densities.

The charge-discharge curves of the ACs in 1 M H_2SO_4 solution at different current densities were shown in Figure 5. And which could be calculated by the formula:[12, 13]

$$c = \frac{I\Delta t}{\Delta V m}$$

Where C is the specific capacitance ($F \cdot g^{-1}$), I is the charge-discharge current (A), ΔV is 0.5 V, and m is the mass of active material with the electrode.

As illustrated in Figure 5, the charge discharge curve of both 1-AC and 2-AC are symmetrical. It is explained that the two kind of activated carbon is stored energy by electric double layer capacitance. At a current density of 0.2 A/g, the specific capacitance of the 1-AC and 2-AC electrode materials reached the maximum, which were 128 F/g and 235 F/g, respectively. With the increase of current density, their specific capacitance decreased. However, the value of 2-AC was always larger than that of 1-AC. This is because the specific surface area of 2-AC is larger than that of 1-AC, which can adsorb more electrolyte ions for the application as a double layer energy storage [14].

3.5 Stability testing 1-AC and 2-AC

To examine the cycling performance of 1-AC and 2-AC, these ACs were measured by charge-discharge cycling at a current density of 2 $A \cdot g^{-1}$ for 500 cycles. As shown in Figure 6, the results show that the capacity of both 1-AC and 2-AC could maintain more than 90%, indicating good electrochemical reversibility.

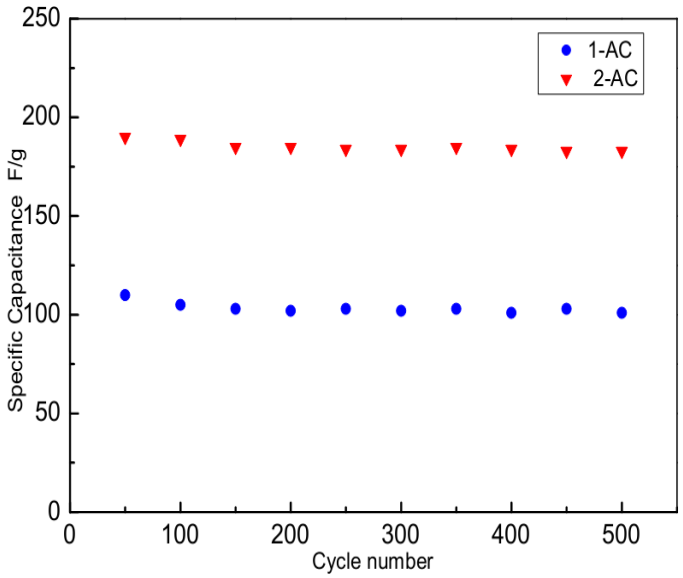

Figure 6. The dependence of the specific capacitance of 1-AC and 2-AC as charge/discharge cycle number.

4. CONCLUSIONS

To sum up, ACs with different specific surface areas were successfully obtained and analysed by physical and electrochemical methods. The electrochemical properties of them were thoughtfully studied. The results prove that the electrochemical performances of AC with larger surface area to volume ratio (1700~1900 m^2/g) were much better than these of smaller surface area to volume ratio (600~800 m^2/g) AC. The stability of the charge and discharge shows that the two ACs electrode materials have good electrochemical stability, and the specific capacitance after 500 cycles is maintained at more than 90%. We believe these results suggest that the AC with larger surface area to volume ratio could be a promising candidate as supercapacitor electrode material.

ACKNOWLEDGEMENTS
We acknowledge the Doctoral Research Fund of Southwest University of Science and Technology (No. 12zx7131).

References

1. S. J. Park, D. W. Kim and J. H. Lee, *J. Nanosci. Nanotechnol.*, 14 (2014) 9263-9267.
2. X.L. Wang, J.J. Li and Z.Y. Yu, *Int. J. Electrochem. Sci.*, 10 (2015) 93-101.
3. N. Shirshova, H. Qian, M. Houlle, J. H. Steinke, A. R. Kucernak, Q. P. Fontana, E. S. Greenhalgh, A. Bismarck and M. S. Shaffer, *Faraday Discuss.* 172 (2014) 81-103.
4. Y. F. Nie, Q. Wang, X. Y. Chen and Z. J. Zhang, *Phys. Chem. Chem. Phys.*, 18 (2016) 2718-2729.
5. A. Elmouwahidi, Z. Zapata-Benabithe, F. Carrasco-Marin and C. Moreno-Castilla, *Bioresour. Technol.*, 111 (2012) 185-90.
6. T. Kim, G. Jung, S. Yoo, K. S. Suh and R. S. Ruoff, *ACS Nano*, 7 (2013) 6899-6905.

7. G. Wang, H. Wang, X. Lu, Y. Ling, M. Yu, T. Zhai, Y. Tong and Y. Li, *Adv. Mater.*, 26 (2014), 2676-2682.
8. C. Largeot, C. Portet, J. Chmiola, P. L. Taberna, Y. Gogotsi and P. Simon, *J. Am. Chem. Soc.*, 130 (2008) 2730-2731.
9. H. J. Liu, X. M. Wang, W. J. Cui, Y. Q. Dou, D. Y. Zhao and Y. Y. Xia, *J. Mater. Chem.*, 20 (2010) 4223-4230.
10. L. L. Zhang, X. Zhao, M. D. Stoller, Y. Zhu, H. Ji, S. Murali, Y. Wu, S. Perales, B. Clevenger and R. S. Ruoff, *Nano lett.*, 12 (2012) 1806-1812.
11. D. Saha, Y. Li, Z. Bi, J. Chen, J. K. Keum, D. K. Hensley, H. A. Grappe, H. M. Meyer, 3rd, S. Dai, M. P. Paranthaman and A. K. Naskar, Langmuir 30 (2014), 900-910.
12. R. R. Salunkhe, Y. H. Lee, K. H. Chang, J. M. Li, P. Simon, J. Tang, N. L. Torad, C. C. Hu and Y. Yamauchi, *Chemistry*, 20 (2014) 13838-13852.
13. T. J. Trivedi, D. Bhattacharjya, J. S. Yu and A. Kumar, *ChemSusChem*, 8 (2015) 3294-3303.
14. L. Deng, R. J. Young, I. A. Kinloch, A. M. Abdelkader, S. M. Holmes, D. A. De Haro-Del Rio and S. J. Eichhorn, *ACS Appl. Mater. Interfaces*, 5 (2013) 9983-9990.